SUPPLEMENTARY MATERIAL

Bauhinia forficata Link extract attenuates insulin resistance by preserving glucose uptake in *gastrocnemius* muscle

Patricia Gasparini[a], Ingrid Candido Garofolo[a], Monica Marques Telles[a], Lila Missae Oyama[b], Viviane de Mello Veneza[c], Thiago André Moura Veiga[c], Vera Lucia Flor Silveira[a] and Luciana Chagas Caperuto[a,*].

[a]*Departamento de Ciências Biológicas, Universidade Federal de São Paulo (UNIFESP), Rua Arthur Riedel, 275, Bairro Eldorado, 09972-270, Diadema, SP, Brazil.*
[b]*Departamento de Fisiologia, Escola Paulista de Medicina, Universidade Federal de São Paulo (UNIFESP), Rua Botucatu, 862, Vila Clementino, 04023-901, São Paulo, SP, Brazil.*
[c]*Departamento de Química, Universidade Federal de São Paulo (UNIFESP), Rua Arthur Riedel, 275, Bairro Eldorado, 09972-270, Diadema, SP, Brazil.*

*Corresponding author**:** Luciana Chagas Caperuto.
Tel.: ++55 11 40440500 R 3474.
E-mail address: caperuto@unifesp.br (L.C. Caperuto)

ABSTRACT

Bioactive metabolites from *Bauhinia forficata* Link (Bf extract) hold therapeutic potential for type 2 diabetes mellitus (T2DM) but the mechanism remains poorly understood. This study aimed to test the extract from Bf leaves obtained by decoction on the prevention of T2DM *in vivo*. The Bf extract was tested on a streptozotocin-induced T2DM mouse model fed on a high-fat diet. The insulin resistance was attenuated in T2DM animals supplemented with Bf extract, which indicates glucose intolerance reduction and p-AKT/AKT ratio preservation in the *gastrocnemius* muscle. These observations suggested that Bf extract enhanced glucose uptake. Nevertheless, there was no preservation in β-cell insulin secretion in Bf extract-treated T2DM mice. Interestingly, the Bf extract reduced body weight gain without affecting total energy intake. Hence, Bf extract has a hypoglycemic effect which could attenuate the development of insulin resistance**.**

Keywords: decoction, streptozotocin, high-fat diet, Kaempferitrin, p-AKT/AKT, hypoglycemic effect, insulin resistance.

Materials

- Accu-Check glucometer (Roche, São Paulo, Brazil).
- Anti-5' adenosine monophosphate-activated protein kinase (AMPK) antibody (code 2603, Cell Signaling Technology; Danvers, USA).
- Anti-AKT antibody (9272, Cell Signaling Technology; Danvers, USA).
- Anti-c-Jun N-terminal kinase (JNK) antibody (code 9252, Cell Signaling Technology; Danvers, USA).
- Anti-extracellular signal–regulated kinases (ERK1/2) antibody (code 9102, Cell Signaling Technology; Danvers, USA).
- Anti-phosphorylated 5' adenosine monophosphate-activated protein kinase (p-AMPK) (code 2531, Cell Signaling Technology; Danvers, USA).
- Anti-phosphorylated AKT (p-AKT) antibody (Ser-473, code 9271, Cell Signaling Technology; Danvers, USA).
- Anti-phosphorylated c-Jun N-terminal kinase (p-JNK) antibody (9251, Cell Signaling Technology; Danvers, USA).
- Anti-phosphorylated extracellular signal–regulated kinases (p-ERK1/2) antibody (code 9101, Cell Signaling Technology; Danvers, USA).
- AxioVision Software (Axiocam, Carl Zeiss, Oberkochen, Germany).
- Centrifuge 5810 R (Eppendorf, Hamburg, Germany).
- Creatinine test (code 35, Labtest Diagnóstica, São Paulo, Brazil).
- Diode array detector (DAD) (SPD-M20A, Shimadzu, Tokyo, Japan).
- Enzyme-linked immmunosorbent assay (ELISA) (EZRMI-13K, Merck Millipore, Darmstadt, Germany).
- Folin & Ciocalteu's phenol reagent (Sigma-Aldrich, Saint Louis, USA).
- Food to mice (Nuvilab, São Paulo, Brazil).
- Formic acid formol (formaldehyde, Labsynth, São Paulo, Brazil).
- Freezone 2.5L Freeze Dry System (Labconco, Kansas City, USA).
- Gallic acid (code 3170, Vetec, São Paulo, Brazil).
- Glutamate-pyruvate transaminase (GPT) test (code 53, Labtest Diagnóstica, São Paulo, Brazil).
- Glutamic-oxaloacetic transaminase (GOT) test (code 52, Labtest Diagnóstica, São Paulo, Brazil).
- High-density lipoprotein (HDL) cholesterol test (code 13, Labtest Diagnóstica, São Paulo, Brazil).
- High-Performance Liquid Chromatography (LC-6AD, Shimadzu, Tokyo, Japan).

- Insulin (Novolin R; Novo Nordisk A/S, São Paulo, Brazil).
- Metanol CAS 67-56-1 (Merck Millipore, São Paulo, Brazil).
- Microscope (Primo Vert, Carl Zeiss, Oberkochen, Germany).
- Monohydrated citric acid (code A1027, Labsynth, São Paulo, Brazil).
- Reverse phase column (Phenyl-Hexyl, 150 x 0.46 mm, Luna® 5 µm, Torrance, USA).
- Sodium dodecyl sulfate polyacrylamide gel electrophoresis (SDS-PAGE, Bio-Rad, Hercules, EUA).
- Cube Gel Electrophoresis Mini-protean (Bio-Rad, Hercules, EUA).
- Streptozotocin N-(Methylnitrosocarbamoyl)-α-D-glucosamine (Sigma-Aldrich, Saint Louis, USA).
- Thiopental sodium (THIOPENTAX®, Cristália, São Paulo, Brazil).
- Total cholesterol (TC) test (code 76, Labtest Diagnóstica, São Paulo, Brazil).
- Total protein test (code 99, Labtest Diagnóstica, São Paulo, Brazil).
- Triacylglycerol (TAG) test (code 87, Labtest Diagnóstica, São Paulo, Brazil).
- Trisodium citrate dihydrate (code C1033, Labsynth, São Paulo, Brazil).
- Ultrapure water (Milli-Q® Reference, Merck Millipore, Darmstadt, Germany).
- UVI Band Software (UVITEC, Cambridge, UK).

Experimental

Ethical approval

The present study was performed following experimental protocols approved by the Ethics Committee on the Use of Animals at the *Universidade Federal de São Paulo* (#4125110914), which is under the guidelines of the "Guide for the Care and Use of Laboratory Animals" (NIH Publications No. 8023, revised 1978).

Bf aqueous extract

Leaves from Bf were collected in August 2015, at the Institute of Botany of São Paulo (IBt). This time of the year corresponds to the winter season in the Southern Hemisphere. Plants were previously identified, and a voucher specimen was deposited (#454737) at the IBt herbarium, in 2014. Aqueous leaf extracts were prepared by decoction, according to Lino *et al*. (2004). Briefly, 1kg of fresh leaves was boiled in 6 L of water for 30 min and filtered. The resulting extract was transferred to bottles and maintained at -20°C. When required, the content was freeze-dried by a freeze-dry system (Labconco, Kansas City, USA), solubilized in drinking water, and administered by gavage. The plant name was checked against the Plant List (http://www.theplantlist.org).

Total flavonoid and polyphenol contents

Total flavonoid content in the Bf extract was determined using the Dowd method (Meda et al., 2005), and was expressed as µg of quercetin equivalents per mg of Bf extract (µg QE.mg^{-1}).

Total polyphenol content was determined using the Folin–Ciocalteu colorimetric method (Singleton et al., 1999), and was expressed as µg of gallic acid equivalents per mg of Bf extract (µg GAE.mg^{-1}).

Chromatographic analysis

High-Performance Liquid Chromatography (HPLC) was employed to separate the compounds present in the Bf extract, and to detect the kaempferol-3,7-*O*-(α)-dirhamnoside (Kaempferitrin). Briefly, 2 mg of freeze-dried Bf extract was solubilized in 2 mL of 50% MeOH (Merck Millipore, Darmstadt, Germany) and injected into the HPLC instrument (LC-6AD, Shimadzu, Tokyo, Japan), which was equipped with a diode array detector (DAD) (SPD-M20A, Shimadzu, Japan) and a reverse-phase column (Phenyl-Hexyl, 150 x 0.46 mm, Luna® 5 µm). The analytical method utilized an isocratic elution mode with a 1.0 mL.min^{-1} flow, employing 20% MeOH in 80% ultrapure water. For the detection of kaempferitrin, the ultraviolet (UV) spectra obtained for each chromatographic peak were compared to the spectra of *Bauhinia rufa* leaves, which served as the standard.

Animals

Six-month-old male C57Bl/6J mice (n=69), from the Center for Development of Experimental Models at *Universidade Federal de São Paulo*, were housed, two mice per cage, with environmental enrichment, in a controlled area. This area was maintained at 25°C, with a 12 h light/dark cycle, and the mice were provided with food (Nuvilab, São Paulo, Brazil) and water *ad libitum*. Animals were randomly divided into four groups: control with normal fat diet (10% kcal) group supplemented with water (C); control supplemented with Bf by oral gavage (CBf); high-fat diet (60% kcal) and streptozotocin (HS); and high-fat diet and streptozotocin supplemented with Bf by oral gavage (HSBf). Each group contained 16 to 18 animals. The composition of normal fat and high-fat diets is described in Table S1.

Body weight (BW) and 24-hour food intake were evaluated twice a week and the values were normalized with 10 g of BW. Energy intake was calculated by multiplying the food intake (g) by 3.82 kcal, for a normal fat diet, and 5.24 kcal for a high-fat diet (HFD). Energy efficiency was calculated by the ratio between body weight gain (g) and energetic intake (kcal).

Table S1. Components and proportions of the diets

	Normal Fat Diet		***High Fat Diet* (HFD)**	
Ingredients	**g/100g**	**Kcal**	**g/100g**	**Kcal**
Casein	18.96	800	25.84	800
L-cystine	0.28	12	0.39	12
Corn starch	28.86	1260	0	0
Maltodextrin 10	3.32	140	16.15	500
Sucrose	33.17	1400	8.89	275.2
Microcrystalline Cellulose	4.74	0	6.46	0
Corn oil	2.37	225	3.23	225
Pork fat	1.89	180	31.66	2205
Mineral mix AIN 93#	0.95	0	1.29	0
Dibasic potassium phosphate	1.23	0	1.68	0
Calcium carbonate	0.52	0	0.71	0
Potassium citrate	1.56	0	2.13	0
Vitamin mix 93##	0.95	40	1.29	40
Colina Bitartrate	0.19	0	0.26	0
	g (%)	**kcal (%)**	**g (%)**	**kcal (%)**
Protein	19	20	26	20
Carbohydrate	67	70	26	20
Fat	4	10	35	60
kcal/g	3.82		5.24	

#Mineral Mix (100g): Boron 1.426 mg, Calcium 14.294 g, Chlorine 4.490 g, Copper 17.241 mg, Chromium 2.885 mg, Sulfur 860 mg, Iron 100 mg, Fluorine 2.872 mg, Phosphorus 5.690 g, Iodine 0.593 mg, Lithium 0.285 mg, Magnesium 1.448 g, Manganese 30 mg, Molybdenum 0.432 mg, Nickel 1.431 mg, Potassium 10.286 g, Selenium 0.428 mg, Silicon 14.326 mg, Sodium 2.938 mg, Vanadium 0.287 mg, Zinc 86 mg. ##Vitamin Mix (100g): Folic Acid 40 mg, Nicotinic Acid 600 mg, Biotin 4 mg, Vitamin B5 64 mg, Vitamin B6 140 mg, Riboflavin 120 mg, Vitamin B1 12 mg, Vitamin A 80,000 IU, Vitamin B12 520 mg, Vitamin D3 20,000 IU, Vitamin E 1500 IU, Vitamin K1 15 mg.

Experimental design and prevention of T2DM

After one week of the acclimation period, the four groups were fed a normal fat diet or HFD (Gilbert et al., 2011). Simultaneously, CBf and HSBf mice were administered 200 mg of Bf kg^{-1} of body weight (BW) once a day, by oral gavage (Lino et al., 2004). The Bf extract solution for gavage was freshly prepared, by resuspending the dry extract in 200µL of drinking water. The same volume of water, without Bf, was administered to C and HS mice by gavage. This procedure was repeated daily for 6 weeks. To extrapolate the BF dose to humans (Reagan-Shaw et al., 2007), the surface area of the human body was considered. Thus, a dose of 200 $mg.kg^{-1}$ BW of Bf is

equivalent to 16 $mg.kg^{-1}$ BW to humans, which corresponds to a daily dose of 1.12g for 70kg individuals.

Three weeks after initiating the diet and gavage procedures, the HS and HSBf mice were fasted for 6 hours and then administered 1 intraperitoneal (ip) injection of low-dose STZ (40 $mg.kg^{-1}$ BW), diluted in the vehicle (0.1M cold citrate buffer, pH 4.5), for 3 consecutive days. This protocol was previously shown to induce partial β-cell deficiency (Gilbert et al., 2011). Under the same conditions, mice from the C and CBf groups were administered 100 µL of vehicle. The streptozotocin (STZ) was prepared fresh each day and administered at 4 p.m. One week after the first injection, HS and HSBf mice were administered a higher dose of STZ (90 $mg.kg^{-1}$ BW), and C and CBf mice were administered 100 µL of vehicle, by ip. The fasting glycemia was measured on euthanasia day and mice with a glycemia of greater than 230 $mg.dL^{-1}$ were considered to be diabetic.

At the end of the experimental period, mice were fasted for 12h and anesthetized with an injection of thiopental sodium (60 $mg.kg^{-1}$ BW). Blood was collected from the retro-orbital plexus, and centrifuged at 2,204×g, at 4°C, for 10 min, and the separated serum was stored at -80°C. Animals were euthanized with supplemental anesthesia and subcutaneous and visceral fat depots (epididymal and retroperitoneal - RET), liver, pancreas, and *gastrocnemius* muscle, were carefully collected, weighed and immediately stored at -80°C. The tissue weight was normalized by 10 g of body weight (BW) and the weight of visceral fat depots was used to calculate visceral adiposity.

The retroperitoneal depot, liver, and *gastrocnemius* muscle are insulin targets that contribute to the glucose homeostasis. The hind limb *gastrocnemius* muscle is a large skeletal muscle composed of heterogeneous populations of muscle fibers. Normal male C56BL/6 mice gastrocnemius has around 25% of oxidative fibers, composed of type I (slow-twitch) fibers and type IIa fibers (fast-oxidative fibers), and roughly 70% of glycolytic fibers, composed of type IIb (fast-glycolytic fibers) (Augusto et al., 2004; Julien, Bordeau et al., 2018). It is also an insulin target frequently analyzed in T2DM animal models (Zanuto et al., 2013; Lima et al, 2006; Campbell et al., 2004; Lima et al, 1998; Fueger et al., 2004).

Blood parameters

Triacylglycerol (TAG), total cholesterol (TC), high-density lipoprotein (HDL) cholesterol, total protein, creatinine, glutamic-oxaloacetic transaminase (GOT), and glutamate-pyruvate transaminase (GPT) were quantified using commercially available assay~~s~~ kits (Labtest Diagnóstica, Brazil). The non-HDL cholesterol concentrations were calculated based on the following equation: non-HDL ($mg.dL^{-1}$) = TC – HDL. Insulin levels were measured using an enzyme-linked immunosorbent assay (ELISA) (EZRMI-13K, Millipore, USA). The homeostatic model assessment index (HOMA-β) was used to estimate β-cell function, through the following

formula with fasting values: HOMA-β = [20 × fasting blood insulin ($\mu U.mL^{-1}$)/ (fasting blood glucose ($mmol.L^{-1}$) – 3.5)].

Oral Glucose Tolerance Test (oGTT) and Intraperitoneal Insulin Tolerance Test (ipITT)

Glucose and insulin tolerance tests were made in all animals, in the early part and middle of week 6, of the experimental period, respectively. For the oGTT, mice received glucose by gavage (1 $g.kg^{-1}$ BW) after a 12h fasting period. Blood was collected by a tail incision before (0 min) and 15, 30, 60, 90, and 120 min after the glucose gavage, and then analyzed using an Accu-Check glucometer (Roche, São Paulo, Brazil). The area under the curve (AUC) was determined from the analysis of the glucose concentration values and time data.

For the ipITT, mice fasted overnight and subsequently injected with insulin (Novolin R; Novo Nordisk A/S, Denmark; 0,75 $U.kg^{-1}$ BW). Glucose measurements were determined before (0 min) and 5, 10, 15, 20, 25, and 30 min after the insulin injection. The AUC was determined from the analysis of the glucose concentrations and time to insulin resistance data.

Histological analysis

Pancreatic tissue (n=5-6) was collected after perfusion with 4% formaldehyde. The head of the pancreas was separated, fixed in 4% formaldehyde-fixing solution. The tissue was then sectioned and stained with hematoxylin and eosin (H&E) at Histotech (São Paulo, Brazil). Islet area was measured (μm^2) using a 20X objective lens of an optical microscope (Primo Vert, Carl Zeiss, Germany) and the AxioVision Software (Axiocam, Carl Zeiss, Germany). Only islets with an average area of greater than 10,000 μm^2 were considered for this evaluation.

Protein extraction and western blotting analysis

Protein extraction and western blot analyses were performed according to Caperuto et al. (2008). Following sodium dodecyl sulfate-polyacrylamide gel electrophoresis (SDS-PAGE) and western blot transfer, the membranes were incubated overnight at 4°C with primary antibody against total protein kinase B, also known AKT (9272), phosphorylated AKT (p-AKT) (Ser-473, 9271), phosphorylated extracellular signal-regulated kinases (p-ERK1/2) (9101), extracellular signal-regulated kinases (ERK1/2) (9102), phosphorylated c-Jun N-terminal kinase (p-JNK) (9251), c-Jun N-terminal kinase (JNK) (9252), phosphorylated 5' adenosine monophosphate-activated protein kinase (p-AMPK) (2531) or 5' adenosine monophosphate-activated protein kinase (AMPK) (2603), (Cell Signaling Technology; Danvers, MA, EUA). Enhanced chemiluminescence (ECL) (450µM p-coumaric acid, 5.4mM hydrogen peroxide, 100µM Tris, pH 8.5, 2.5mM luminol) was used for signal development, and detected bands were analyzed and quantified using the UVI Band Software (UVITEC, Cambridge, UK). All the results are expressed

in arbitrary units (AU). Total protein was used as the control for each respective phosphorylated form of the proteins since the same membrane was used again after stripping

Statistical analysis

Results are expressed as means ± standard error of the mean (SEM). All data were analyzed with a normality test (D'Agostino-Pearson) and linear correlation coefficient (>20%). Non-parametric analysis (fasting insulinemia, HOMA-β index, and islets area) was performed using the Kruskal-Wallis test followed by a *post hoc* Dunn for multiple comparisons test. Parametric statistical analysis (body weight, energy intake, tissues weight, oGTT, ipITT, fasting glycemia, blood measurement, and protein phosphorylation) were performed using two-way analysis of variance (ANOVA) with a *post hoc* Tukey multiple comparison test. Results were considered statistically significant at $p<0.05$ and as a trend at $p<0.1$. Graph Pad Prism 7 software was used to analyze all the data.

Figures captions

Figure S1. Reversed-phase chromatography, Peak 1 represents the most polar compound, with each subsequent peak/compound being slightly less polar. (A) Bf extract chromatographic profile analysis (peaks 1-5) and retention time (RT). (B) Chromatographic profile analysis from Kaempferitrin standard isolated from *B. rufa*. (C) UV Kaempferitrin spectrum. (D) Enlarged Bf chromatogram (peaks 2-5). (E) UV spectrum corresponding to peak 5 of Bf chromatogram (RT=17.84 min).

Figure S2. Bf extract effects on glucose intolerance and insulin resistance. (A) Oral glucose tolerance test (oGTT). (B) Area under the curve (AUC) for oGTT. (C) Insulin tolerance test (ipITT). (D) AUC for ipITT. (E) Fasting glycemia. (F) Fasting insulinemia. (G) HOMA-β index. Results were analyzed by two-way ANOVA and Tukey's post-hoc tests (A-E) and Kruskal-Wallis and Dunn's post-hoc tests (F and G). Values are represented as mean ± standard error of the mean (SEM). n=11-18 (A and B); n=10-18 (C-E); n=4-8 (F and G). *$p<0.05$ *vs.* C; $^{\#}p<0.05$ *vs.* CBf; $^{\$}p<0.05$ *vs.* HS; $^{T}p=0.09$ *vs.* HS (B); $^{T}p=0.081$ *vs.* HS (C); $^{T}p=0.063$ *vs.* C (G).

Figure S3. Impact of Bf extract on islet area in T2DM mice. (A) Islets area (μm^2). Representative photomicrographs (H&E) of islet morphology in different experimental groups: (B) C. (C) CBf. (D) HS. (E) HSBf. Results were analyzed by Kruskal-Wallis and Dunn's post-hoc tests. Values are represented as mean ± standard error of the mean (SEM). n=5-6. C and CBf received a citrate buffer by intraperitoneal injection. HS and HSBf received STZ diluted in citrate buffer by intraperitoneal injection. Horizontal bar=50μm.

Figure S4. Influence of Bf extract in ERK, AKT and AMPK phosphorylation for T2DM partial prevention. (A) Representative images of each target phosphorylation. (B) Total protein used as control for each phosphorylated target. Results were analyzed by two-way ANOVA and Tukey's post-hoc tests. Values are represented as mean ± standard error of the mean (SEM). n=10-17 (pERK/ERK and pAKT/AKT–liver); n=4-9 (pERK/ERK and pAKT/AKT–*gastrocnemius* and RET; pAMPK/AMPK - liver, *gastrocnemius* and RET). *$p<0.05$ *vs.* C; $^{\$}p<0.05$ *vs.* HS. RET: retroperitoneal fat depot.

Figure S5. Effects of Bf extract in JNK phosphorylation for T2DM partial prevention. (A) Representative images of target phosphorylation. (B) Total protein used as control for each phosphorylated target. Results were analyzed by two-way ANOVA and Tukey's post-hoc tests. Values are represented as mean ± standard error of the mean (SEM). n=4-9. $^{T}p=0.068$ *vs.* CBf (liver); $^{T}p=0.051$ *vs.* CBf (*gastrocnemius*). RET: retroperitoneal fat depot.

Figure S6. Effects of Bf extract on body composition and energy intake. (A) Body weight. (B) Total body weight gain. (C) Total energy intake. (D) Energy efficiency. Results were analyzed by two-way ANOVA and Tukey's post-hoc tests. Values are represented as mean ± standard error of the mean (SEM). n = 16-18. *$p<0.05$ *vs.* C; $^{\#}p<0.01$ *vs.* CBf; $^{T}p=0.071$ *vs.* HS (C).

Figures

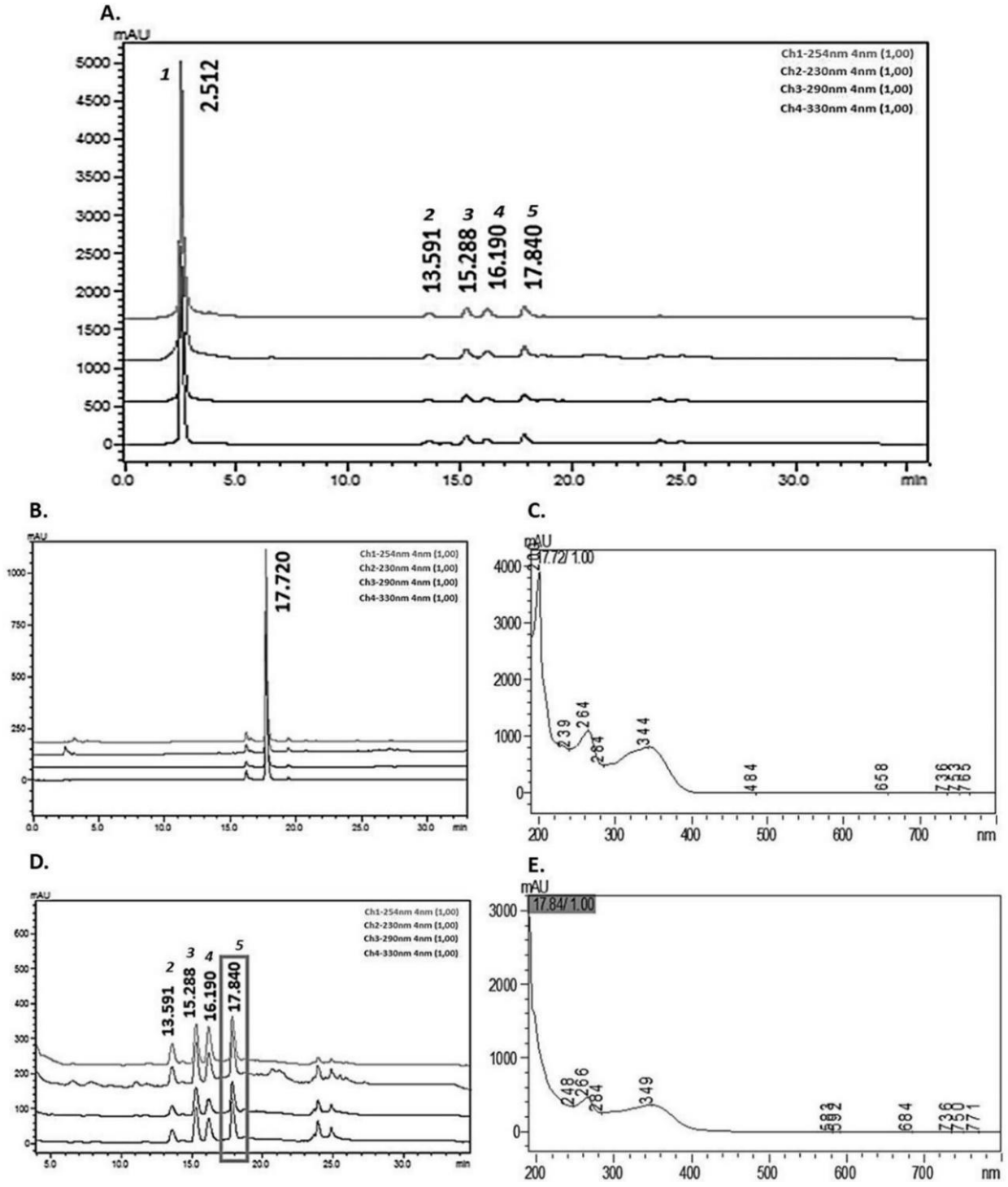

Figure S1. Reversed-phase chromatography, Peak 1 represents the most polar compound, with each subsequent peak/compound being slightly less polar. (A) Bf extract chromatographic profile analysis (peaks 1-5) and retention time (RT). (B) Chromatographic profile analysis from Kaempferitrin standard isolated from *B. rufa*. (C) UV Kaempferitrin spectrum. (D) Enlarged Bf chromatogram (peaks 2-5). (E) UV spectrum corresponding to peak 5 of Bf chromatogram (RT=17.84 min).

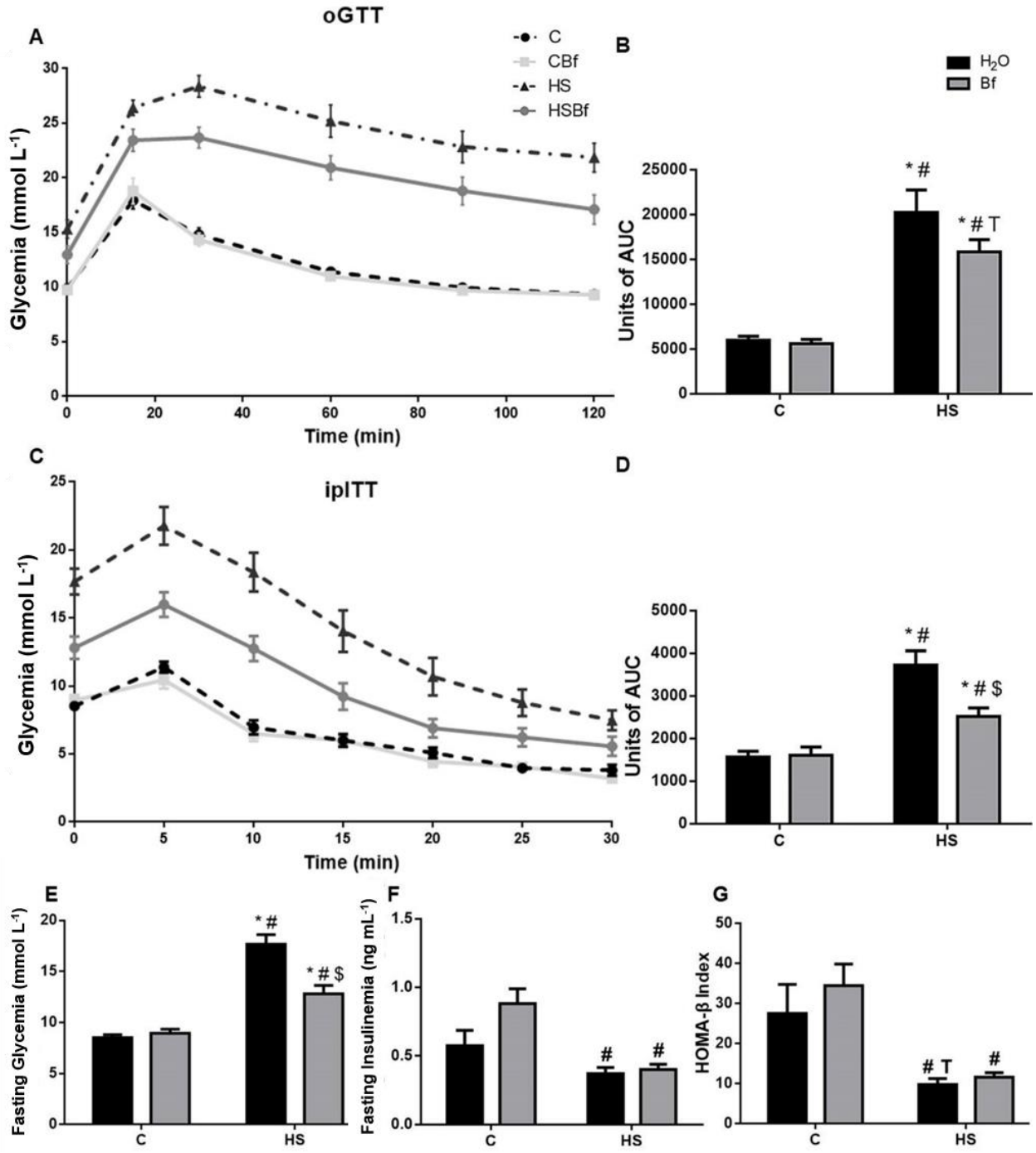

Figure S2. Bf extract effects on glucose intolerance and insulin resistance. (A) Oral glucose tolerance test (oGTT). (B) Area under the curve (AUC) for oGTT. (C) Insulin tolerance test (ipITT). (D) AUC for ipITT. (E) Fasting glycemia. (F) Fasting insulinemia. (G) HOMA-β index. Results were analyzed by two-way ANOVA and Tukey's post-hoc tests (A-E) and Kruskal-Wallis and Dunn's post-hoc tests (F and G). Values are represented as mean ± standard error of the mean (SEM). n=11-18 (A and B); n=10-18 (C-E); n=4-8 (F and G). *$p<0.05$ *vs.* C; $^{\#}p<0.05$ *vs.* CBf; $^{\$}p<0.05$ *vs.* HS; $^{T}p=0.09$ *vs.* HS (B); $^{T}p=0.081$ *vs.* HS (C); $^{T}p=0.063$ *vs.* C (G).

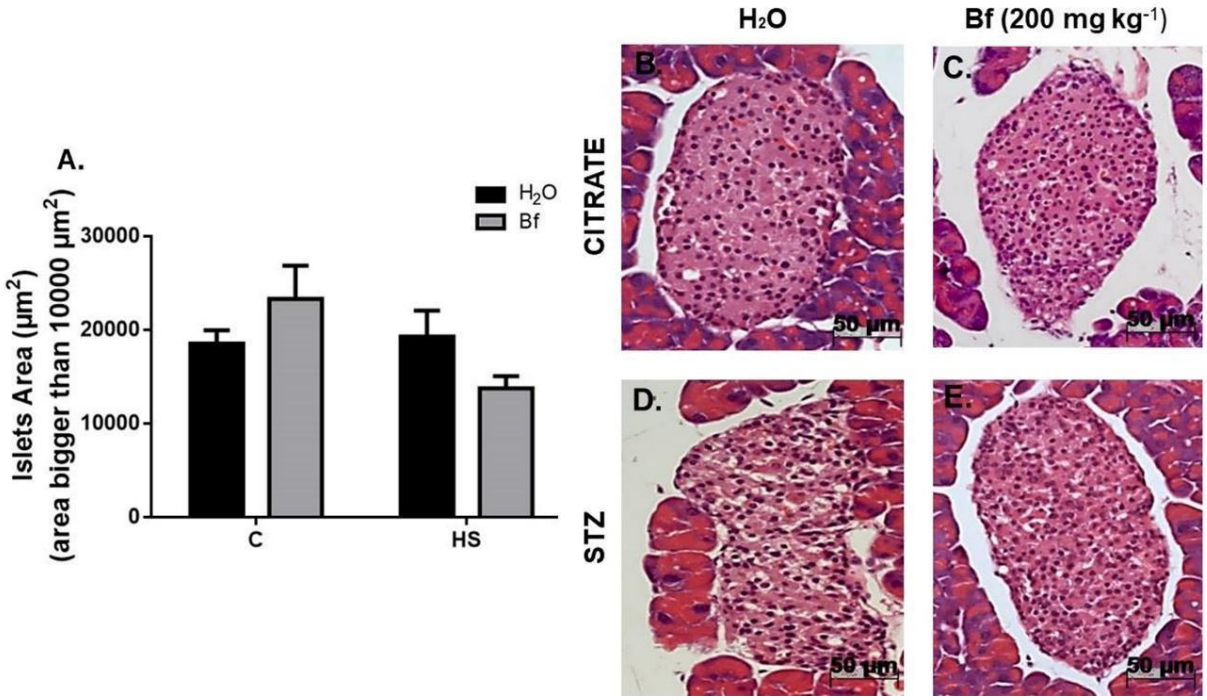

Figure S3. Impact of Bf extract on islet area in T2DM mice. (A) Islets area (µm^2). Representative photomicrographs (H&E) of islet morphology in different experimental groups: (B) C. (C) CBf. (D) HS. (E) HSBf. Results were analyzed by Kruskal-Wallis and Dunn's post-hoc tests. Values are represented as mean ± standard error of the mean (SEM). n=5-6. C and CBf received a citrate buffer by intraperitoneal injection. HS and HSBf received STZ diluted in citrate buffer by intraperitoneal injection. Horizontal bar=50µm.

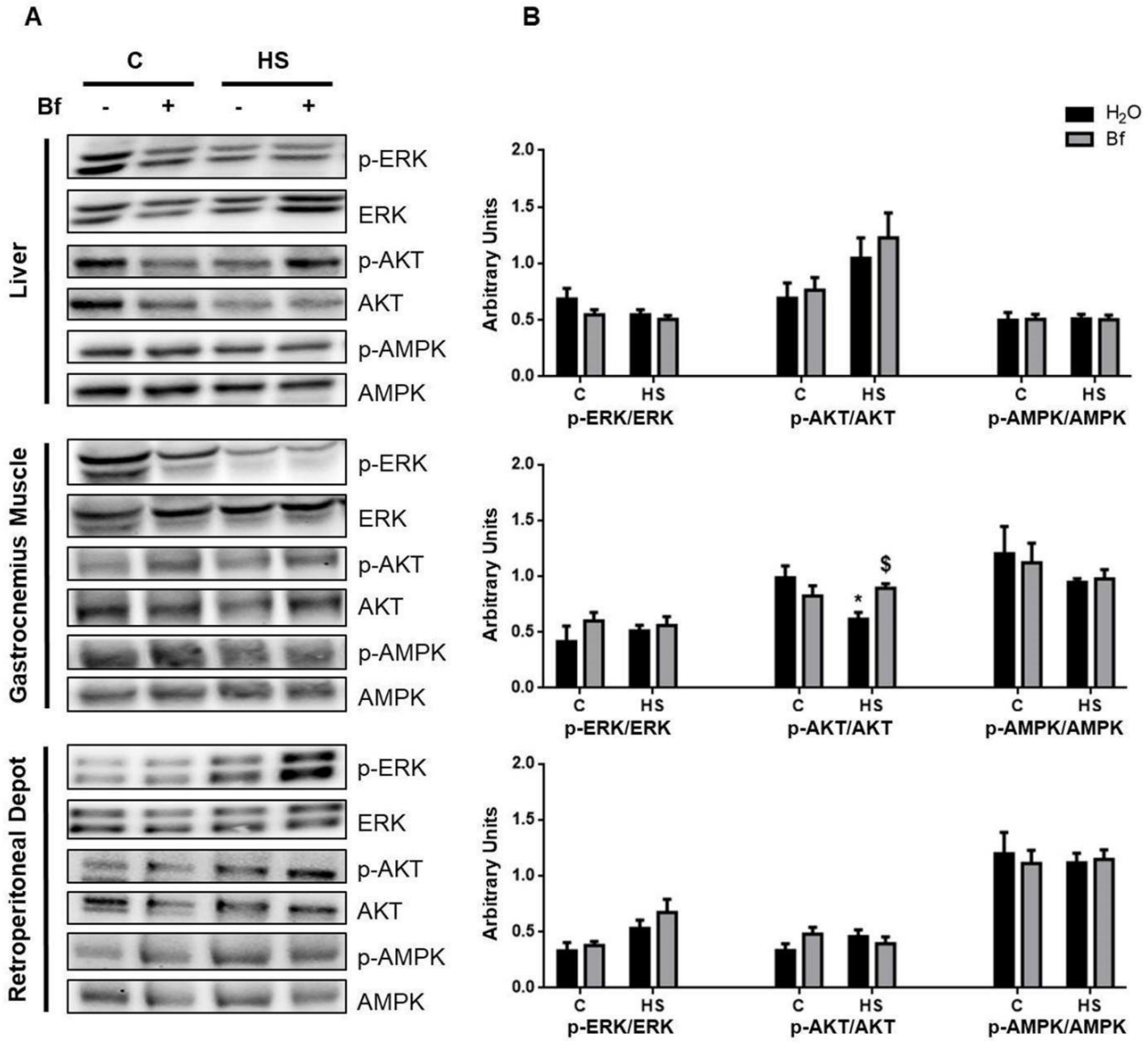

Figure S4. Influence of Bf extract in ERK, AKT and AMPK phosphorylation for T2DM partial prevention. (A) Representative images of each target phosphorylation. (B) Total protein used as control for each phosphorylated target. Results were analyzed by two-way ANOVA and Tukey's post-hoc tests. Values are represented as mean ± standard error of the mean (SEM). n=10-17 (pERK/ERK and pAKT/AKT–liver); n=4-9 (pERK/ERK and pAKT/AKT–*gastrocnemius* and RET; pAMPK/AMPK - liver, *gastrocnemius* and RET). *$p<0.05$ *vs.* C; $^{\$}p<0.05$ *vs.* HS. RET: retroperitoneal fat depot.

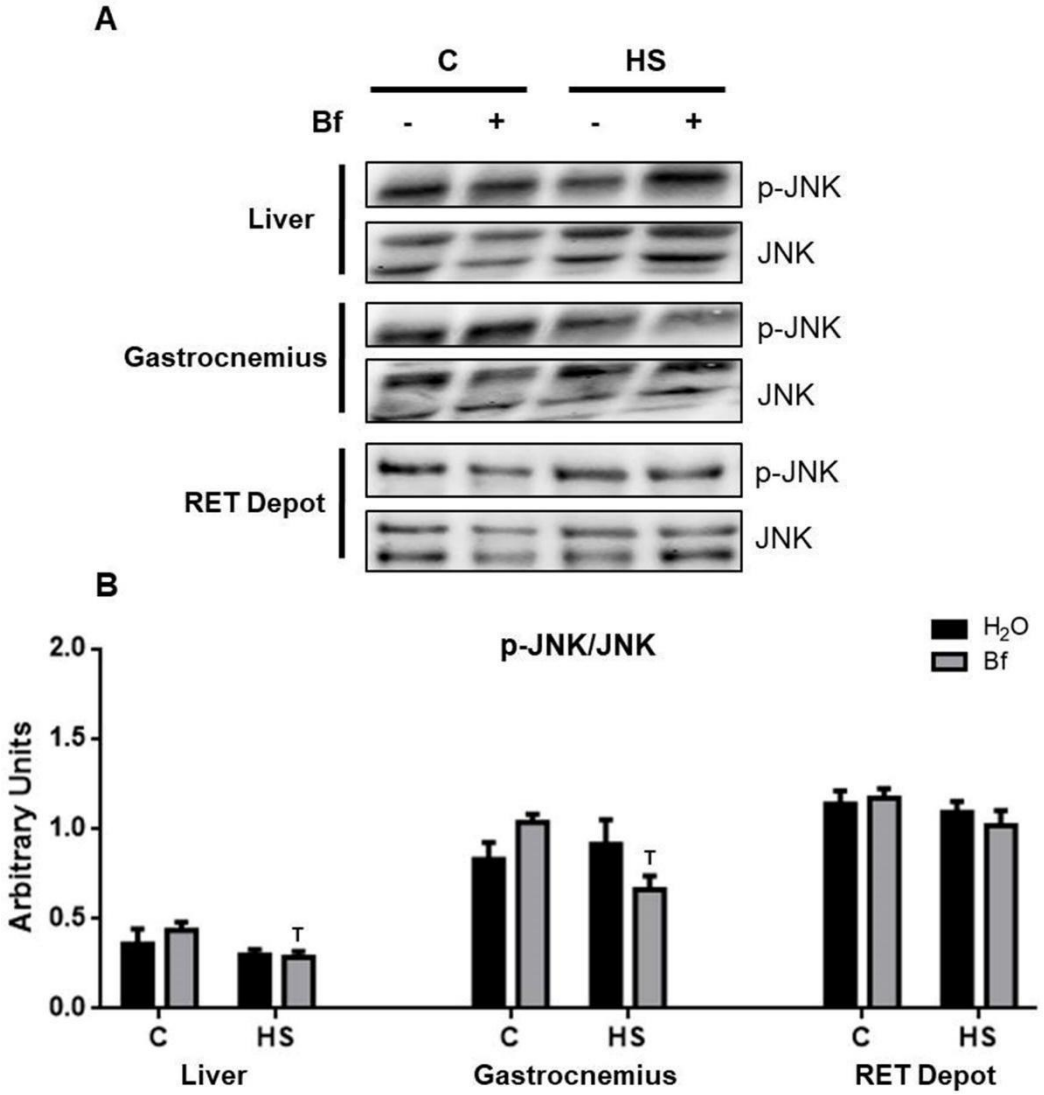

Figure S5. Effects of Bf extract in JNK phosphorylation for T2DM partial prevention. (A) Representative images of target phosphorylation. (B) Total protein used as control for each phosphorylated target. Results were analyzed by two-way ANOVA and Tukey's post-hoc tests. Values are represented as mean ± standard error of the mean (SEM). n=4-9. ^{T}p=0.068 *vs.* CBf (liver); ^{T}p=0.051 *vs.* CBf (*gastrocnemius*). RET: retroperitoneal fat depot.

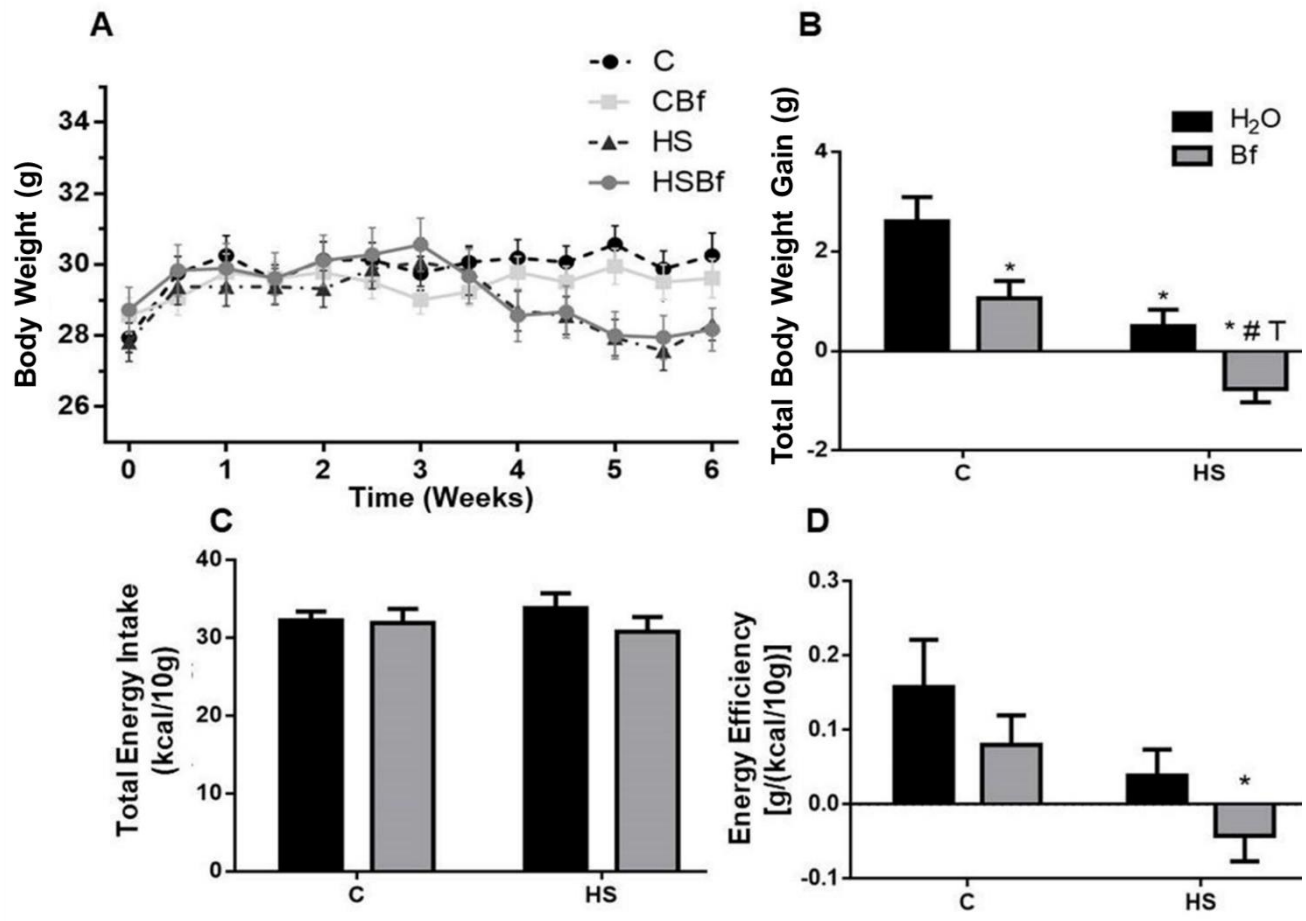

Figure S6. Effects of Bf extract on body composition and energy intake. (A) Body weight. (B) Total body weight gain. (C) Total energy intake. (D) Energy efficiency. Results were analyzed by two-way ANOVA and Tukey's post-hoc tests. Values are represented as mean ± standard error of the mean (SEM). n = 16-18. *$p<0.05$ *vs.* C; $^{\#}p<0.01$ *vs.* CBf; $^{T}p=0.071$ *vs.* HS (C).

Tables captions

Table S2. Total flavonoid and polyphenol contents in 1 $mg.mL^{-1}$ of Bf extract.

Table S3. Liver, *gastrocnemius* muscle, subcutaneous and visceral fat weight ($mg.10g\ BW^{-1}$). n=6-13.

Table S4. Blood testing. n=10-17.

Tables

Table S2. Total flavonoid and polyphenol contents in 1 mg.mL^{-1} of Bf extract.

	Total Flavonoid	**Total Polyphenol**
(µg.mL^{-1})	21.83	40.92
(g.g dried sample^{-1})	0.022	0.041

Table S3. Liver, *gastrocnemius* muscle, subcutaneous and visceral fat weight (mg.10g BW^{-1}). n=6-13.

Weight (mg.10g BW^{-1})	**C**	**CBf**	**HS**	**HSBf**
Liver	382.6 ± 15	392.8 ± 12.5	409.5 ± 12.7	400.9 ± 9.9
***Gastrocnemius* Muscle**	102.2 ± 0.3	97.5 ± 7.8	100.8 ± 5.0	94.7 ± 3.1
Subcutaneous Depot	154.4 ± 22	142.7 ± 8.7	129.5 ± 10	123.5 ± 6.7
Retroperitoneal Depot	81.1 ± 14.7	66.5 ± 5.5	83.1 ± 7.3	65.6 ± 5.8
Epididymal Depot	251.7 ± 32.8	224.7 ± 12.5	251.3 ± 20.7	197.5 ± 17
Visceral Adiposity	332.9 ± 46.7	285.9 ± 17.7	334.4 ± 27.1	270.6 ± 20.7

Results were analyzed by two-way ANOVA and Tukey's post-hoc tests. Values are represented as mean ± standard error of the mean (SEM).

Table S4. Blood testing. n=10-17.

	C	**CBf**	**HS**	**HSBf**
Triglycerides (mg.dL^{-1})	52.5 ± 5.4	44.9 ± 3.7	50 ± 4.2	40.4 ± 3.4
Total Cholesterol (mg.dL^{-1})	134.3 ± 5.8	133.8 ± 5.9	128 ± 8.2	140.9 ± 5.6
HDL Cholesterol (mg.dL^{-1})	127.5 ± 3.9	122.7 ± 5.3	107.2 ± 6.5	113.9 ± 4
non-HDL (mg.dL^{-1})	29.2 ± 11.5	24.5 ± 5.1	22.1 ± 4.1	31.2 ± 5.3
Total Protein (g.dL^{-1})	10.1 ± 0.8	8.8 ± 0.7	8.7 ± 0.8	8 ± 0.6
GPT (U.mL^{-1})	25.9 ± 4.7	11.2 ± 2.3*****	29.5 ± 3.6 **#**	15.7 ± 1.7 **$**
GOT (U.mL^{-1})	77.8 ± 9.5	73.9 ± 8.9	89.4 ± 7.6	70.3 ± 7.2
Creatinine (mg.dL^{-1})	0.3 ± 0.08	0.2 ± 0.03	0.2 ± 0.2	0.2 ± 0.03

*p<0.05 *vs.* C; $^{\#}$p<0.05 *vs.* CBf; $^{\$}$p<0.05 *vs.* HS. Results were analyzed by two-way ANOVA and Tukey's post-hoc tests. Values are represented as mean ± standard error of the mean (SEM). GOT: glutamic oxaloacetic transaminase enzyme, GPT: glutamate pyruvate transaminase enzyme.

References

Augusto V, Padovani CR, Campos GER. Skeletal Muscle Fiber Types in C57BL/6J Mice. Braz. J. morphol. Sci. 2004 21(2), 89-94.

Bourdeau Julien I, Sephton CF, Dutchak PA. Metabolic Networks Influencing Skeletal Muscle Fiber Composition. Front Cell Dev Biol. 2018 Sep 28;6:125. doi: 10.3389/fcell.2018.00125. PMID: 30324104; PMCID: PMC6172607.

Campbell CS, Caperuto LC, Hirata AE, Araujo EP, Velloso LA, Saad MJ, Carvalho CR. The phosphatidylinositol/AKT/atypical PKC pathway is involved in the improved insulin sensitivity by DHEA in muscle and liver of rats in vivo. Life Sci. 2004 Nov 19;76(1):57-70. doi: 10.1016/j.lfs.2004.06.017. PMID: 15501480.

Caperuto, L.C., Anhê, G.F., Cambiaghi, T.D., Akamine, E.H., do Carmo Buonfiglio, D., Cipolla-Neto, J,, Curi, R., Bordin, S., 2008. Modulation of bone morphogenetic protein-9 expression and processing by insulin, glucose, and glucocorticoids: possible candidate for hepatic insulin-sensitizing substance. Endocrinology. 149, 6326-6335.

Fueger PT, Hess HS, Bracy DP, Pencek RR, Posey KA, Charron MJ, Wasserman DH. Regulation of insulin-stimulated muscle glucose uptake in the conscious mouse: role of glucose transport is dependent on glucose phosphorylation capacity. Endocrinology. 2004 Nov;145(11):4912-6. doi: 10.1210/en.2004-0465. Epub 2004 Jul 29. PMID: 15284204.

Gilbert, E.R., Fu, Z., Liu, D., 2011. Development of a Nongenetic Mouse Model of Type 2 Diabetes. Experimental Diabetes Research, Volume 2011, Article ID 416254, 12 pages.

Lima FB, Machado UF, Bartol I, Seraphim PM, Sumida DH, Moraes SM, Hell NS, Okamoto MM, Saad MJ, Carvalho CR, Cipolla-Neto J. Pinealectomy causes glucose intolerance and decreases adipose cell responsiveness to insulin in rats. Am J Physiol. 1998 Dec;275(6):E934-41. doi: 10.1152/ajpendo.1998.275.6.E934. PMID: 9843734.

Lima MH, Souza LC, Caperuto LC, Bevilacqua E, Gasparetti AL, Zanuto R, Saad MJ, Carvalho CR. Up-regulation of the phosphatidylinositol 3-kinase/protein kinase B pathway in the ovary of rats by chronic treatment with hCG and insulin. J Endocrinol. 2006 Aug;190(2):451-9. doi: 10.1677/joe.1.06226. PMID: 16899578.

Lino, C.S., Diogenes, J.P., Pereira, B.A., Faria, R.A., Andrade Neto, M., Alves, R.S., De Queiroz, M.G., De Sousa, F.C., Viana, G.S., 2004. Antidiabetic activity of *Bauhinia forficata* extracts in alloxan-diadetic rats. Biol Pharm Bull 27, 125-27.

Meda, A., Lamien, C.E., Romito, M., Millogo, J., Nacoulma, O.G., 2005. Determination of the total phenolic, flavonoid and proline contents in Burkina Fasan honey, as well as their radical scavenging activity. Food Chem 91, 571-577.

Reagan-Shaw, S., Nihal, M., Ahmad, N., 2007. Dose translation from animal to human studies revisited. The FASEB Journal 22, 659-661.

Singleton, V.L., Orthofer, R., Lamuela-Raventos, R.M., 1999. Analysis of total phenols and other oxidation substrates and antioxidants by means of Folin-Ciocalteu reagent. Methods Enzymol. 299, 152-178.

Zanuto R, Siqueira-Filho MA, Caperuto LC, Bacurau RF, Hirata E, Peliciari-Garcia RA, do Amaral FG, Marçal AC, Ribeiro LM, Camporez JP, Carpinelli AR, Bordin S, Cipolla-Neto J, Carvalho CR. Melatonin improves insulin sensitivity independently of weight loss in old obese rats. J Pineal Res. 2013 Sep;55(2):156-65. doi: 10.1111/jpi.12056. Epub 2013 Apr 9. PMID: 23565768.